

DOI: 10.1002/cbic.201402100

DNA-Scaffolded Multivalent Ligands to Modulate Cell Function

Zhiqing Zhang,^[a, b] Mark A. Eckert,^[b] M. Monsur Ali,^[b] Linan Liu,^[b] Dong-Ku Kang,^[b] Elizabeth Chang,^[b] Egest J. Pone,^[b] Leonard S. Sender,^[c] David A. Fruman,^[d] and Weian Zhao*^[b]

We report a simple, versatile, multivalent ligand system that is capable of specifically and efficiently modulating cell-surface receptor clustering and function. The multivalent ligand is made of a polymeric DNA scaffold decorated with biorecognition ligands (i.e., antibodies) to interrogate and modulate cell receptor signaling and function. Using CD20 clustering-mediated apoptosis in B-cell cancer cells as a model system, we demonstrated that our multivalent ligand is significantly more effective at inducing apoptosis of target cancer cells than its monovalent counterpart. This multivalent DNA material approach represents a new chemical biology tool to interrogate cell receptor signaling and functions and to potentially manipulate such functions for the development of therapeutics.

Cell-surface receptors play essential roles in cellular function and in the interplay between cells and their extracellular environment. Intriguingly, cell-surface receptors do not always work alone but rather can assemble into higher order dimeric or oligomeric complexes that function cooperatively.^[1,2] In particular, multivalency is a key principle in many biological interactions in nature. Multivalent interactions between cell-surface receptors and their ligands are critical to enhance functional binding affinity and selectivity and to modulate biological signaling through ligand-induced receptor clustering.^[1,2] Inspired

by nature, chemists have synthesized multivalent materials, including linear polymers, dendrimers, and nanoparticles that are modified with multiple ligands to study and modulate cell-surface receptor signaling and to eventually develop new therapeutics.^[1–3] For instance, pioneering work from Kiessling's group has demonstrated that neoglycopolymers bearing L-selectin-binding carbohydrates (i.e., sialyl Lewis X derivatives), synthesized by ring-opening metathesis polymerization, can promote L-selectin clustering and subsequent shedding of leukocytes.^[4] Kopeček and colleagues have synthesized an antibody-conjugated *N*-(2-hydroxypropyl)methacrylamide (HPMA) polymer backbone, which binds to cell-surface receptors (i.e., CD20) to mediate downstream cellular signaling (i.e., apoptosis) through multivalent clustering.^[5–8] Although these examples demonstrate the feasibility of modulating cell-receptor clustering and signaling by using synthetic multivalent materials, current methods to prepare multivalent systems are complex and often involve chemistries that are not easily modified.

We recently exploited a new class of one-dimensional DNA molecules, synthesized by an efficient isothermal enzymatic reaction called rolling circle amplification (RCA),^[9–12] which not only embrace advantages of nucleic acids as material building blocks (e.g., highly predictable and reprogrammable base pairing and engineering versatility)^[13–16] but are particularly suited for the development of multivalent synthetic ligands. In RCA, DNA polymerase (e.g., phi29 DNA polymerase) extends DNA from a primer in the presence of deoxynucleotide triphosphates (dNTPs) by replicating a circular DNA template many times to yield single-stranded (ss) DNA products containing repeating sequence units that can enable multivalent, cooperative binding. The RCA products are complementary to the circular DNA template and, therefore, their sequences can be tailored to accommodate compositions including aptamer sequences, spacer domains, and restriction enzyme sites.^[9–12] Additionally, functional moieties (e.g., dyes, biotin, and nanoparticles) on the nucleic acid backbones can be introduced by chemical or enzymatic synthesis or by hybridization with short complementary strands, and can be positioned with exceptional accuracy.^[13–16] We recently utilized RCA to produce multivalent aptamers for targeted drug delivery to cancer cells and capture of cancer cells from solutions.^[11,12] In these studies, we demonstrated that RCA products containing multiple aptamer units surpass their monovalent counterparts with respect to cancer cell binding affinity and efficiency due to their cooperative, multivalent effects.

[a] Prof. Dr. Z. Zhang

State Key Laboratory of Heavy Oil Processing
College of Science, China University of Petroleum
66 Changjiang (West) Rd, Huangdao, Qingdao, 266580 (P. R. China)

[b] Prof. Dr. Z. Zhang, Dr. M. A. Eckert, Dr. M. M. Ali, L. Liu, Dr. D.-K. Kang,


E. Chang, Dr. E. J. Pone, Prof. Dr. W. Zhao
Department of Pharmaceutical Sciences
Department of Biomedical Engineering
Sue and Bill Gross Stem Cell Research Center and
Chao Family Comprehensive Cancer Center, and
Edwards Lifesciences Center for Advanced Cardiovascular Technology
University of California, Irvine
845 Health Sciences Road, Irvine, CA 92697 (USA)
E-mail: weianz@uci.edu
Homepage: <http://faculty.sites.uci.edu/zhaolab/>

[c] Prof. Dr. L. S. Sender

Department of Medicine, University of California, Irvine
Hyundai Cancer Institute, CHOC Children's Hospital
1201 W. La Veta Avenue, Orange, CA 92697 (USA)

[d] Prof. Dr. D. A. Fruman

Department of Molecular Biology & Biochemistry, University of California
3242 McLaugh Hall, Irvine, CA 92697 (USA)

 Supporting information for this article is available on the WWW under <http://dx.doi.org/10.1002/cbic.201402100>.

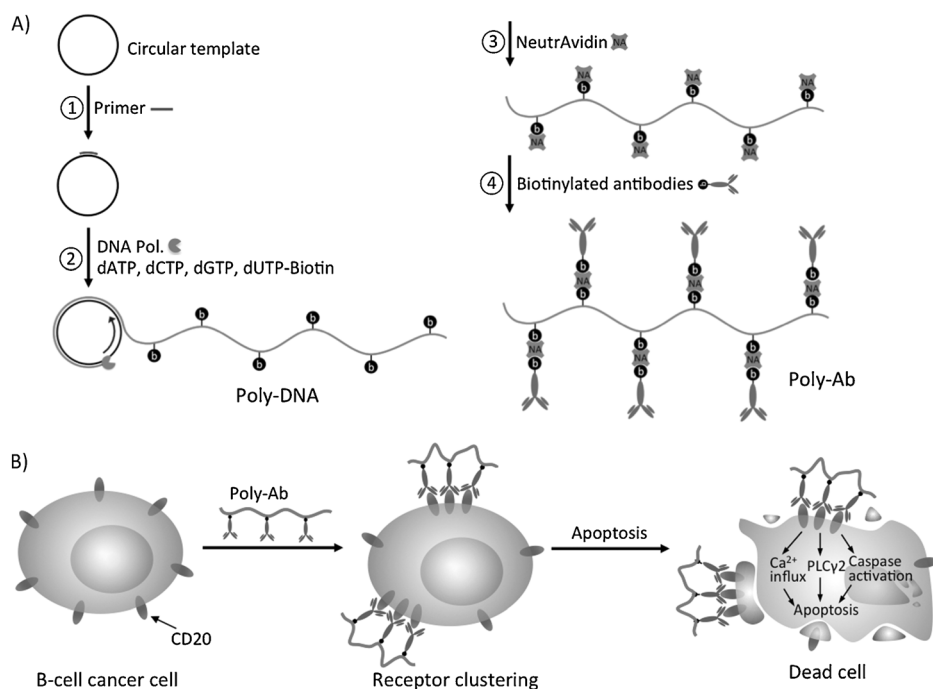


Figure 1. A) Construction of a multivalent DNA scaffold that carries multiple antibodies (Poly-Ab). The Poly-Ab is composed of a repetitive DNA sequence synthesized by rolling circle amplification and containing multiple biotins to facilitate binding to biotinylated antibodies through a NeutrAvidin-based linkage. B) The Poly-Ab modulates cellular receptor signaling via multivalency-mediated effects. Specifically, the clustering of CD20 receptors on B-cell cancer cell surfaces by the CD20 Poly-Ab leads to activation of multiple downstream pathways, culminating in induction of apoptosis.

In this study, we hypothesized that the DNA molecules synthesized by RCA (referred to as “Poly-DNA”, Figure 1A) can serve as a simple polymeric scaffold to immobilize biorecognition ligands (e.g., antibodies, aptamers, and carbohydrates) in a highly defined and programmable manner, functioning as multivalent ligands to interrogate and modulate cell receptor function. To test this hypothesis, we chose well-established CD20 clustering-induced apoptosis in B-cell cancer cells as a model system. CD20 ligation induces several well-characterized signaling events, beginning with a dramatic intracellular influx of calcium ions (Ca^{2+}), subsequent phosphorylation of phospholipase C gamma 2 (PLC γ 2), and caspase activation that culminates in induction of apoptosis.^[5–8, 17–20] B-cell lymphoma and leukemia, especially non-Hodgkin’s lymphoma (NHL) and chronic lymphocytic leukemia (CLL), are among the most prevalent cancers.^[21] Recently, monoclonal antibodies, including Rituximab, that target the B-cell-specific antigen, CD20, have been used to treat CD20-positive B-cell cancers.^[17–20] Although anti-CD20 antibodies have demonstrated promising results, the drug has limited ability to induce direct apoptosis in its monovalent form, due to its inefficiency at clustering CD20 receptors.^[5–8, 17–20]

Herein, we report a novel multivalent ligand system composed of simple DNA molecular scaffolds (Poly-DNA) on which multiple anti-CD20 antibodies are assembled (“Poly-Ab”; Figure 1A). The system is composed of a repetitive DNA sequence containing multiple biotins to facilitate binding to biotinylated antibodies through a NeutrAvidin-based linkage. The long DNA

molecules were synthesized by using RCA in the presence of deoxynucleotide triphosphates (dNTPs) and biotinylated deoxyuridine triphosphates (biotin-dUTPs) from a primer replicating a circular DNA template using phi29 DNA polymerase (Figure 1A). The RCA product is designed to be a Poly-A sequence, which leads to minimal nonspecific intra- and intermolecular base pairing, with biotin-dUTPs incorporated at defined positions. Successful synthesis of the RCA product was confirmed by agarose gel electrophoresis (Figure S1). In our experience, an RCA reaction carried out according to our procedure typically yields products containing approximately 50 repeating units. The CD20 Poly-Ab molecules in the RCA product were synthesized by bridging the biotin molecules in the RCA product with biotinylated mouse anti-human CD20 antibodies (or control IgG) through NeutrAvidin. To verify and quantify antibody incorporation

in the RCA products, we also prepared the Poly-Ab on magnetic beads, which facilitated separation of conjugated products from unreacted reagents. Using fluorescently tagged NeutrAvidin, we first demonstrated that biotin molecules are incorporated into RCA products and are viable to conjugate NeutrAvidin (Figure S2). We then demonstrated that biotin-modified antibodies can be subsequently attached to the NeutrAvidin/RCA product complex, evidenced by the positive staining of a Cy5-tethered secondary antibody (Figure S2). After incubation of the CD20 Poly-Ab-attached beads with fluorescently tagged secondary antibody that binds to CD20 antibody, we measured the fluorescence of bound and unbound secondary antibodies and determined that one Poly-Ab molecule carries approximately nine CD20 antibodies (see the Experimental Section for details).

We next characterized the binding of the CD20 Poly-Ab to CD20+ lymphoma cells using flow cytometry and confocal microscopy. We incubated target CD20+ Ramos cells with CD20 Poly-Ab, control Poly-IgG, or anti-CD20 monoclonal antibody (Mono-Ab). An important control for nonspecific binding also includes an acute lymphoblastic T-cell leukemia cell line (CCRF-CEM) that does not express CD20. Poly-Ab is fluorescently labeled by incorporation of FITC-NeutrAvidin, whereas biotin-modified Mono-Ab was visualized with FITC-NeutrAvidin staining. As shown in Figure 2, we have demonstrated that CD20 Poly-Ab specifically binds to target CD20+ Ramos cells. We also noted that CD20 Poly-Ab tends to form large clusters on the cell surface, whereas Mono-Ab stains cells relatively uni-

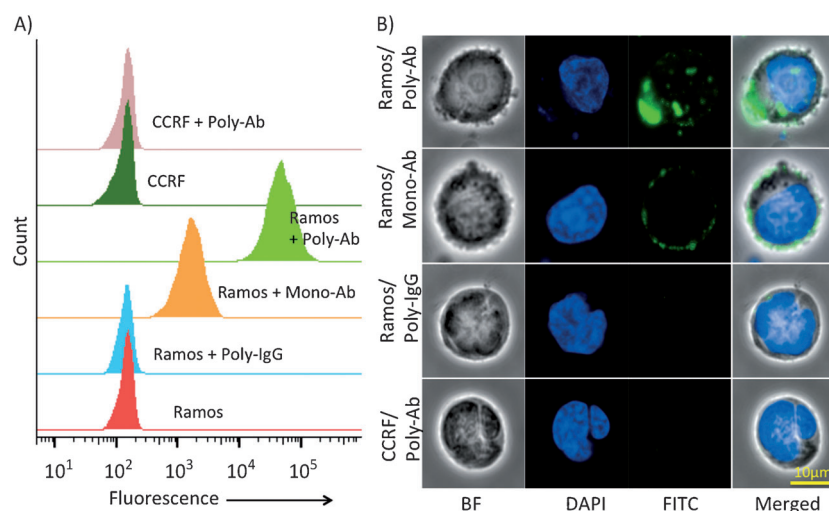


Figure 2. Flow cytometry and confocal microscopy images show that the CD20 Poly-Ab specifically binds to target CD20+ Ramos cells. The Poly-Ab is fluorescently labeled by incorporation of FITC-NeutrAvidin, whereas biotin-modified Mono-Ab is visualized with FITC-NeutrAvidin staining.

formly (Figure 2B). We hypothesized that the Poly-Ab would efficiently and robustly induce clustering of CD20 on the surface of CD20+ Ramos cells. To test this hypothesis, we immunostained the Poly-Ab-bound Ramos cells with an eFluor 660-tagged anti-CD20 antibody, which recognizes an epitope in the cytoplasmic domain and does not compete for the same binding site with the bound CD20 Poly-Ab, to visualize the spatial organization of CD20 on the cell surface and its colocalization with the Poly-Ab or Mono-Ab. Indeed, our data suggest that the Poly-Ab, but not the Mono-Ab, induced CD20 clustering to form large aggregates on the cell surface where CD20 and Poly-Ab are spatially colocalized (Figures 3 and S3). Intriguingly, we often observed that Poly-Ab molecules could assemble multiple cells together (Figure 3, top) likely due to their long, multivalent characteristics.

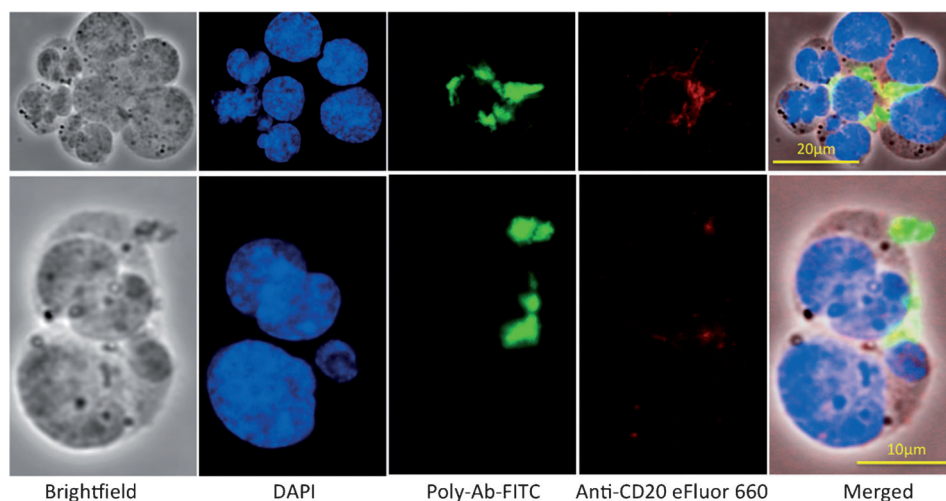


Figure 3. CD20 molecules (red) clustered and colocalized with the CD20 Poly-Ab (green) on the Ramos cell surface. Crosslinking of multiple Ramos cells by the Poly-Ab could be occasionally observed.

Our fundamental hypothesis is that the multivalent nature of the CD20 Poly-Ab will efficiently induce clustering of CD20 on the cell surface to trigger apoptosis in malignant cells (Figure 1B). To determine the specificity, kinetics, and extent of cytotoxicity of the CD20 Poly-Ab, we performed annexin V/propidium iodide (PI) flow cytometry staining of Ramos cells after treatment with the Poly-Ab. Remarkably, our data demonstrate that the CD20 Poly-Ab induces rapid, specific, and effective cell killing effects in a dose-dependent manner with a significantly higher efficiency than the Mono-Ab (Figures 4, 5 and S4). First, the Poly-Ab-induced apoptosis is specific, evidenced by the fact

that the control groups, including Ramos/Poly-IgG and CCRF/CD20, showed minimal toxicity (Figure S4). Given that NeutrAvidin itself might bind to multiple biotin-modified CD20 antibodies to form multivalent antibodies, we included another control (NeutrAvidin-CD20), which was prepared by mixing unbiotinylated RCA products, NeutrAvidin, and biotin-modified CD20 antibodies. We discarded that hypothesis, as the NeutrAvidin-CD20 treatment exhibited only a minimal level of apoptosis compared to the Poly-Ab (Figure S4). We next assessed the kinetics and extent of cytotoxicity of the CD20 Poly-Ab compared to the Mono-Ab. Strikingly, we found that Poly-Ab induced apoptosis of target Ramos cells significantly more rapidly and effectively than Mono-Ab (Figure 4A and B) and in a dose-dependent manner (Figure 4C). For instance, CD20 Poly-Ab and Mono-Ab treatments resulted in approximately 70

and 18% apoptosis at 1 h and 94 and 32% apoptosis at 24 h, respectively. Remarkably, Ramos cells treated with the Poly-Ab for just 1 h led to more apoptotic cells than those treated by Mono-Ab for 24 h. Interestingly, after the rapid initial apoptosis phases (e.g., Figures 4A and 5C, Poly-Ab treatment, 1 h >), Ramos cells treated with CD20 Poly-Ab (but not with Mono-Ab) quickly became necrotic cells, as evidenced by low Annexin and high PI staining in flow cytometry analysis (Figure 4A, 24 h treatment) and by ruptured cell membranes and dissociated nuclei in morphological analyses (Figure 5D, 24 h treatment). This

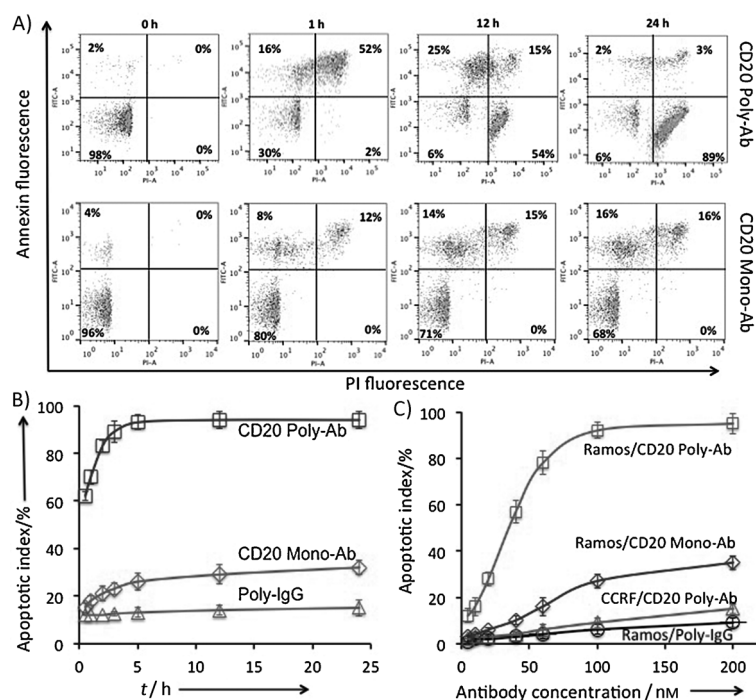


Figure 4. A) and B) Flow cytometry analysis shows that Poly-Ab induces apoptosis of target Ramos cells significantly more rapidly and effectively than Mono-Ab. Viable cells are represented by low annexin and PI staining (lower left), early-stage apoptotic cells are represented by high annexin and low PI staining (upper left), late-stage apoptotic cells are represented by high annexin and high PI staining (upper right), and necrotic cells are represented by high PI and low annexin staining (lower right). The apoptotic index (percentage of apoptotic cells) was derived from flow cytometry annexin V/PI staining. C) Poly-Ab induced apoptosis of target Ramos cells in a specific and dose-dependent manner. Note that the total antibody concentrations in Poly-Ab and Mono-Ab were held constant in order to elucidate the effect of multivalency on cell apoptosis. Error bars in B) and C) were derived from a minimum of three experimental replicates.

dramatic cell killing phenomenon further elaborates the high efficiency of our multivalent system in mediating apoptosis.

In conclusion, we have developed a simple, versatile, multivalent ligand system that is capable of specifically and efficiently modulating cell-surface receptor clustering and apoptosis. Using CD20 clustering-mediated apoptosis in B-cell cancer cells as a model system, we have demonstrated that the multivalent CD20 Poly-Ab is significantly more effective at inducing apoptosis of target Ramos cells than its monovalent counterpart (Mono-Ab). We believe our multivalent DNA material approach represents a new chemical biology tool to interrogate cell receptor signaling and functions. In particular, the versatility of the Poly-DNA system will allow us to incorporate a number of variables which would otherwise be difficult to achieve in other multivalent ligand systems (e.g., neo-glycopolymers), including the number, density, type, position and spatial organization of attached ligands. We anticipate that this will allow measurement and modulation of cell-surface receptor function in a highly defined manner. For instance, the length of the RCA backbone (valency) and distance between antibodies (ligand density) can be easily modified by RCA reaction time and the length of spacer domains between biotin molecules, respectively.^[11,12] In addition, our system has great poten-

tial to incorporate multiple types of ligands (e.g., rituximab and ofatumumab antibodies) that target different cell signaling (e.g., killing, in this study) mechanisms simultaneously.^[17]

We are currently examining our Poly-Ab system in an animal model of lymphoma with respect to its therapeutic efficiency and tumor localization. Importantly, a number of issues must be addressed before it can be considered for future therapeutics: 1) antibody therapy has been clinically used for cancer treatment (e.g., anti-CD20 IgG1 antibody (rituximab) for B-cell lymphoma, anti-HER2 IgG1 antibody (Herceptin) for breast cancer, etc.), most of which belong to the IgG class^[22] and cross the vasculature efficiently within hours to days after IV injection.^[23–25] Nevertheless, one can also use small nanobodies or Fab domains that can effectively access their targets *in vivo*.^[26] 2) Although little is known about the stability of this new class of polymeric DNA structures with respect to nuclease degradation *in vivo*, their stability can be enhanced by incorporation of modified nucleotides and backbone (e.g., phosphorothioate) during the RCA reaction, which is well-established in the area of nucleic acid therapy.^[27] 3) It will also be interesting to investigate how these highly negatively charged polymeric structures extravasate across blood vessels and target cancer cells *in vivo*. Previous studies have demonstrated that negatively charged RNA aptamers can penetrate blood brain barrier *in vivo*.^[28] In addition, Tan and co-workers have demonstrated that highly negatively charged “DNA nano-train” structures can transport drugs to tumors *in vivo*.^[29] Furthermore, nucleic acid therapeutics can be delivered through a variety of vesicles (e.g., liposomes) in order to efficiently cross biological barriers.^[30] 4) Although avidin and its analogues are immunogenic, it has been demonstrated that their immunogenicity does not necessarily constitute a health hazard.^[31] In addition, the immunogenicity of avidin and its analogues can be reduced by PEGylation.^[32] Most importantly, a variety of simple chemical approaches can be utilized to conjugate ligands on the DNA product containing nucleotides modified with functional moieties such as aminoallyl instead of biotin.^[33] 5) Finally, future work will also examine the potential immunogenicity of our Poly-Ab. Given that certain repeated DNA segments containing unmethylated CpG dinucleotides (CpG oligodeoxynucleotides) can provoke immune responses under certain conditions, future studies might employ CpG-free DNA scaffolds, as well as methylated cytosines, which are known to be nonimmunogenic, even in the context of CpG motifs.^[34] On the other hand, the long DNA molecules with tunable length, sequence, and structures could be engineered to induce a desirable immune response for the future development of immunotherapeutics and vaccines.^[35,36]

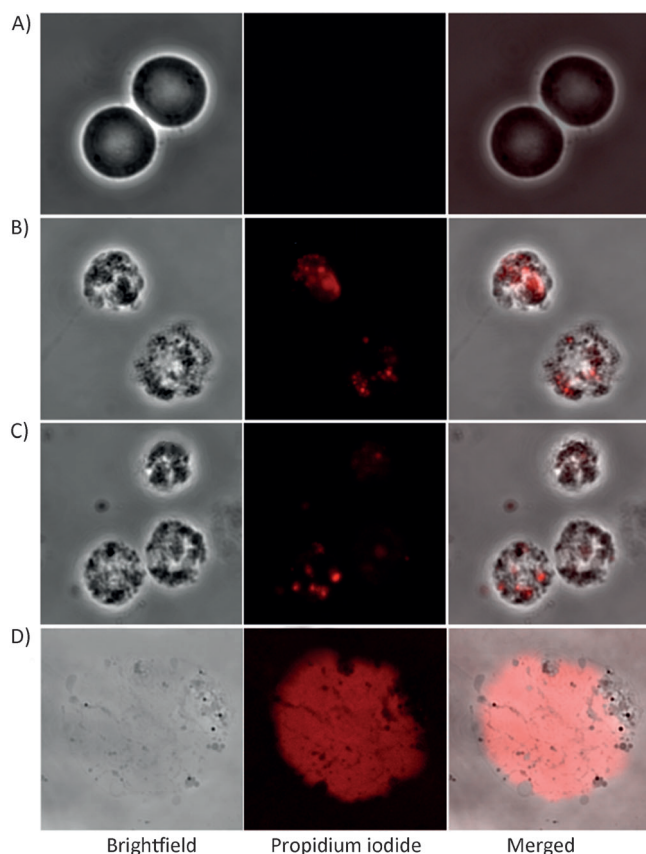


Figure 5. Confocal morphological analysis of Ramos cells A) untreated, B) treated with CD20 Mono-Ab for 24 h, C) treated with CD20 Poly-Ab for 1 h, and D) treated with CD20 Poly-Ab for 24 h. Dead cells were visualized by nuclear PI staining.

Experimental Section

Materials: All DNA (names and sequences in Table S1) were obtained from Integrated DNA Technologies. CCRF-CEM (human acute lymphoblastic leukemia) and Ramos cells (human Burkitt's lymphoma) were purchased from ATCC. RPMI-1640 was purchased from Gibco, and fetal bovine serum (FBS) was obtained from Atlantic Biologicals. Penicillin–streptomycin, SYBR Safe, and FITC annexin V/PI cell apoptosis kits were purchased from Invitrogen. PBS was obtained from Lonza. Circular DNA templates for RCA reactions were synthesized by a template-mediated T4 ligase reaction according to a previously established protocol.^[9] GeneRuler 1 kb plus DNA Ladder, enzymes (T4 polynucleotide kinase, DNA T4 ligase and phi29 DNA polymerase, including the respective tenfold reaction buffers), dNTPs (dATP, dCTP, dGTP, and dTTP), biotin-11-dUTP, NeutrAvidin biotin-binding protein and NeutrAvidin-FITC were obtained from Thermo Scientific. Agarose was purchased from Amresco. Streptavidin magnetic beads were purchased from Bang's Laboratories. Anti-human CD20 biotin and anti-human CD20 eFluor 660 were purchased from eBioscience. Anti-mouse IgG biotin was obtained from Jackson ImmunoResearch. Alexa Fluor 594 goat anti-mouse IgG antibody was purchased from Life Technologies Corporation.

Rolling circle amplification: Rolling circle amplification (RCA) products (Poly-DNA) were synthesized in solution following a previously established protocol.^[9] Typically, primer (50 pmol), circular template (40 pmol), and tenfold RCA reaction buffer (20 μ L) were

mixed in ultrapure water at room temperature. dNTPs (dATP, dGTP, dCTP and biotin-dUTP) and phi29 DNA polymerase (5 μ L, 50 units) were then added to yield a total volume of 200 μ L. RCA reactions were carried out at 30 $^{\circ}$ C for 10 min and then were heat-deactivated at 60 $^{\circ}$ C for 10 min. We characterized the RCA products by using 0.5% agarose gel electrophoresis, which was stained by SYBR Safe and imaged by using a ChemiDoc XRS+ molecular imager (Bio-Rad).

Preparation of CD20 Poly-Ab: RCA products containing biotin (50 pmol) were purified with a Nanosep 30K device (PALL). NeutrAvidin, with or without FITC modification (NeutrAvidin/biotin, molar ratio = 1:1), was then complexed with biotin RCA products at 30 $^{\circ}$ C for 30 min. Next, biotin-modified antibody (anti-human CD20 or IgG control) was incubated with RCA–NeutrAvidin, typically at a molar ratio of 10:1 for 30 min at room temperature. The Poly-Ab was directly used for subsequent experiments without further purification.

Preparation of CD20 Poly-Ab on beads and quantification of the number of antibodies per RCA product: Biotinylated RCA primer (25 pmol each) hybridized with circular template was immobilized on streptavidin magnetic beads (50 μ L). Based on the binding capacity, 50 μ L of beads can bind 9 pmol of biotin. The excess primer/circle complex was washed with 1 \times phi29 buffer (3 \times 200 μ L). The RCA reaction was then conducted in a 200 μ L reaction volume, as described above. After washing, NeutrAvidin (8 μ L, 100 μ M) was immobilized on the RCA products and washed to remove the excess NeutrAvidin. Next, biotinylated anti-human CD20 (66 pmol) antibody was immobilized onto the RCA product for 30 min at room temperature. After washing, Alexa Fluor 594 goat anti-mouse IgG Ab (66 pmol), a secondary antibody for CD20 Ab, was added, and the mixture was incubated for 1 h at room temperature. We observed that approximately 40% of beads were lost during conjugation; this indicated that the remaining 60% contain approximately 6 pmol of RCA products. Finally, the beads were separated by magnet, and the supernatant containing the free unbound secondary antibodies was collected (100 μ L) in a microwell plate. At the same time, secondary antibody (66 pmol) was dissolved in buffer (100 μ L) and added to another well of the microwell plate to compare the fluorescence intensity. The fluorescent intensity of both samples in the microwell plate was obtained by a fluorescent scanner (GE Typhoon scanner, variable mode) and analyzed by ImageQuant software. Based on the calculation, 82% of the added secondary antibody was consumed by the RCA products on beads; this indicated that each RCA molecule contained nine secondary antibodies.

Cell culture: CCRF-CEM, Jurkat, and Ramos cells were cultured in RPMI-1640 supplemented with 10% FBS and 1% penicillin–streptomycin. Before the experiment, cells were washed once with PBS buffer and resuspended in cell capture buffer (PBS with 1% FBS solution).

Poly-Ab/cell interaction: For confocal microscope experiments, CCRF-CEM or Ramos cells (1×10^6 mL) were incubated with CD20 Poly-Ab, Mono-Ab, or Poly-IgG (50 nM total antibodies) in cell culture medium (200 μ L) at 37 $^{\circ}$ C in 5% CO₂ for 15 min. Cells were washed with PBS, fixed in 4% paraformaldehyde for 15 min, and stained with DAPI for 15 min. Cells were centrifuged at 300 rcf for 5 min and resuspended in Vectashield mounting medium (100 μ L). Cell solution was dropped on a glass microcover and observed by using an FV10i confocal microscope (Olympus). To visualize the colocalization of Poly-Ab and CD20 on Ramos cell surfaces, cells bound with CD20 Poly-Ab or Mono-Ab were resuspended in PBS

(200 μL), fixed in 4% paraformaldehyde, and then permeabilized by using 0.5% Triton X-100. Anti-human CD20 eFluor 660 was then added to stain the cytoplasmic domain of CD20 following the manufacturer's protocol.

Samples for flow cytometry experiments were similarly prepared. Briefly, Ramos or control CCRF-CEM cells were incubated with CD20 Poly-Ab, Mono-Ab, or Poly-IgG for 20 min at room temperature in cell culture medium, followed by washing with PBS buffer three times. The cells were suspended in binding buffer (200 μL) for flow cytometry analysis by using a BD LSR II flow cytometer. The data were analyzed with FlowJo software.

Cell apoptosis: In a typical experiment, CCRF-CEM or Ramos cells (1×10^6 mL) were treated with CD20 Mono-Ab, Poly-Ab, or Poly-IgG at various total antibody concentrations (5–200 nM, Figure 4C) for various durations (0.5–24 h, Figure 4B) in a 24-well plate in cell culture medium. In some experiments, in order to test if the complement components in culture media might induce apoptosis of antibody-tagged Ramos cells, culture media were heated at 56 °C for 30 min to inactivate the complement system. We did not observe any difference between media with or without heat inactivation and therefore exclude the potential contribution of the complement system to cell death in our in vitro system.

Apoptosis was assessed by standard flow cytometric FITC annexin V/PI staining according to the manufacturer's protocol. For confocal microscopy experiments, 1×10^6 mL of CCRF-CEM or Ramos cells were incubated with CD20 Mono-Ab, Poly-Ab, or Poly-IgG (50 nM total antibody concentration) in cell culture medium (200 μL) at 37 °C in 5% CO_2 for 1 h or 24 h. Cells were washed with PBS and stained with PI for 15 min. Cell samples were then prepared and observed on an Olympus FV10i confocal microscope.

Acknowledgements

This work was supported by start-up funds from the Department of Pharmaceutical Sciences at the Sue and Bill Gross Stem Cell Research Center and the Chao Family Comprehensive Cancer Center at University of California Irvine. Z.Z. is supported by the National Natural Science Foundation of China (51103179), the National Science Foundation of Shandong Province, China (ZR2011BL017), the Fundamental Research Funds for the Central Universities, and a scholarship from the China Scholarship Council (CSC 201206455009).

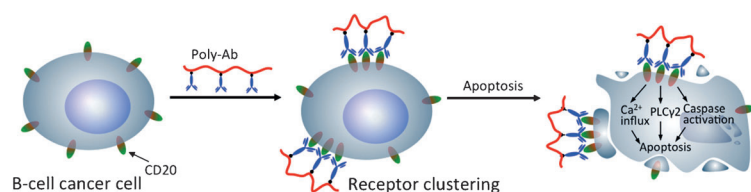
Keywords: cancer • CD20 • DNA nanotechnology • multivalency • rolling circle amplification

- [1] L. L. Kiessling, J. E. Gestwicki, L. E. Strong, *Angew. Chem. Int. Ed.* **2006**, *45*, 2348–2368; *Angew. Chem.* **2006**, *118*, 2408–2429.
- [2] M. Mammen, S. K. Choi, G. M. Whitesides, *Angew. Chem. Int. Ed.* **1998**, *37*, 2754–2794; *Angew. Chem.* **1998**, *110*, 2908–2953.
- [3] Y. F. Huang, H. Liu, X. Xiong, Y. Chen, W. Tan, *J. Am. Chem. Soc.* **2009**, *131*, 17328–17334.
- [4] P. Mowery, Z. Q. Yang, E. J. Gordon, O. Dwir, A. G. Spencer, R. Alon, L. L. Kiessling, *Chem. Biol.* **2004**, *11*, 725–732.
- [5] K. Wu, J. Liu, R. N. Johnson, J. Yang, J. Kopeček, *Angew. Chem. Int. Ed.* **2010**, *49*, 1451–1455; *Angew. Chem.* **2010**, *122*, 1493–1497.
- [6] T. W. Chu, J. Yang, J. Kopeček, *Biomaterials* **2012**, *33*, 7174–7181.
- [7] R. N. Johnson, P. Kopečková, J. Kopeček, *Biomacromolecules* **2012**, *13*, 727–735.
- [8] T. W. Chu, J. Y. Yang, R. Zhang, M. Sima, J. Kopeček, *ACS Nano* **2014**, *8*, 719–731.
- [9] W. Zhao, Y. Gao, S. A. Kandadai, M. A. Brook, Y. Li, *Angew. Chem. Int. Ed.* **2006**, *45*, 2409–2413; *Angew. Chem.* **2006**, *118*, 2469–2473.
- [10] a) W. Zhao, M. M. Ali, M. A. Brook, Y. Li, *Angew. Chem. Int. Ed.* **2008**, *47*, 6330–6337; *Angew. Chem.* **2008**, *120*, 6428–6436; b) M. M. Ali, F. Li, Z. Zhang, K. Zhang, D.-K. Kang, J. Ankrum, C. Le, W. Zhao, *Chem. Soc. Rev.* **2014**, *43*, 3324–3341.
- [11] W. Zhao, C. H. Cui, S. Bose, D. Guo, C. Shen, W. P. Wong, K. Halvorsen, O. C. Farokhzad, G. S. L. Teo, J. A. Phillips, D. M. Dorfman, R. Karnik, J. M. Karp, *Proc. Natl. Acad. Sci. USA* **2012**, *109*, 19626–19631.
- [12] Z. Q. Zhang, M. M. Ali, M. A. Eckert, D. K. Kang, Y. Y. Chen, L. S. Sender, D. A. Fruman, W. Zhao, *Biomaterials* **2013**, *34*, 9728–9735.
- [13] Z. X. Deng, Y. Tian, S. H. Lee, A. E. Ribbe, C. D. Mao, *Angew. Chem. Int. Ed.* **2005**, *44*, 3582–3585; *Angew. Chem.* **2005**, *117*, 3648–3651.
- [14] Z. Cheglakov, Y. Weizmann, A. B. Braunschweig, O. I. Wilner, I. Willner, *Angew. Chem. Int. Ed.* **2008**, *47*, 126–130; *Angew. Chem.* **2008**, *120*, 132–136.
- [15] G. D. Hamblin, K. M. Carneiro, J. F. Fakhoury, K. E. Bujold, H. F. Sleiman, *J. Am. Chem. Soc.* **2012**, *134*, 2888–2891.
- [16] Y. Z. Ma, H. N. Zheng, C. E. Wang, Q. Yan, J. Chao, C. H. Fan, S. J. Xiao, *J. Am. Chem. Soc.* **2013**, *135*, 2959–2962.
- [17] M. S. Czuczman, S. A. Gregory, *Leuk. Lymphoma* **2010**, *51*, 983–994.
- [18] J. K. Hofmeister, D. Cooney, K. M. Coggeshall, *Blood Cells Mol. Dis.* **2000**, *26*, 133–143.
- [19] N. Zhang, L. A. Khawli, P. Hu, A. L. Epstein, *Clin. Cancer Res.* **2005**, *11*, 5971–5980.
- [20] E. A. Rossi, D. M. Goldenberg, T. M. Cardillo, R. Stein, Y. Wang, C. H. Chang, *Cancer Res.* **2008**, *68*, 8384–8392.
- [21] R. Siegel, D. Naishadham, A. Jemal, *Ca-Cancer J. Clin.* **2012**, *62*, 10–29.
- [22] L. M. Weiner, R. Surana, S. Wang, *Nat. Rev. Immunol.* **2010**, *10*, 317–327.
- [23] Z. Xu, H. Zan, E. J. Pone, T. Mai, P. Casali, *Nat. Rev. Immunol.* **2012**, *12*, 517–531.
- [24] E. D. Lobo, R. J. Hansen, J. P. Balthasar, *J. Pharm. Sci.* **2004**, *93*, 2645–2668.
- [25] T. Koleba, M. H. Ensom, *Pharmacotherapy* **2006**, *26*, 813–827.
- [26] S. C. Williams, *Nat. Med.* **2013**, *19*, 1355–1356.
- [27] A. D. Keefe, S. Pai, A. Ellington, *Nat. Rev. Drug Discovery* **2010**, *9*, 537–550.
- [28] C. Cheng, Y. H. Chen, K. A. Lennox, M. A. Behlke, B. L. Davidson, *Mol. Ther. Nucleic Acids* **2013**, *2*, e67.
- [29] G. Zhu, J. Zheng, E. Song, M. Donovan, K. Zhang, C. Liu, W. Tan, *Proc. Natl. Acad. Sci. USA* **2013**, *110*, 7998–8003.
- [30] C. F. Bennett, E. E. Swayze, *Annu. Rev. Pharmacol. Toxicol.* **2010**, *50*, 259–293.
- [31] F. Petronzelli, A. Pelliccia, A. M. Anastasi, R. Lindstedt, S. Manganello, L. E. Ferrari, C. Albertoni, B. Leoni, A. Rosi, V. D'Alessio, K. Deiana, G. Paganelli, R. De Santis, *Cancer Biother. Radiopharm.* **2010**, *25*, 563–570.
- [32] M. Chinol, P. Casalini, M. Maggiolo, S. Canevari, E. S. Omodeo, P. Caliceti, F. M. Veronese, M. Cremonesi, F. Chiolerio, E. Nardone, A. G. Siccardi, G. Paganelli, *Br. J. Cancer* **1998**, *78*, 189–197.
- [33] G. T. Hermanson, *Bioconjugate Techniques*, 2nd ed., Elsevier, Amsterdam, **2008**.
- [34] F. Takeshita, C. A. Leifer, I. Gursel, K. J. Ishii, S. Takeshita, M. Gursel, D. M. Klinman, *J. Immunol.* **2001**, *167*, 3555–3558.
- [35] X. Liu, Y. Xu, T. Yu, C. Clifford, Y. Liu, H. Yan, Y. Chang, *Nano Lett.* **2012**, *12*, 4254–4259.
- [36] J. Li, H. Pei, B. Zhu, L. Liang, M. Wei, Y. He, N. Chen, D. Li, Q. Huang, C. Fan, *ACS Nano* **2011**, *5*, 8783–8789.

Received: March 14, 2014

Published online on ■■■■■, 0000

COMMUNICATIONS



On a roll: DNA molecules synthesized by rolling-circle amplification can serve as simple polymeric scaffolds to interrogate and modulate cell-receptor functions. We have demonstrated that our

multivalent ligand can induce apoptosis of cancer cells more effectively than its monovalent counterpart; this represents a new approach for the development of therapeutics.

Z. Zhang, M. A. Eckert, M. M. Ali, L. Liu, D.-K. Kang, E. Chang, E. J. Pone, L. S. Sender, D. A. Fruman, W. Zhao*



DNA-Scaffolded Multivalent Ligands to Modulate Cell Function

